Fig. 4. Von Kossa staining for visualization of calcifications in cyst walls. Calcifications (calcium deposits) were visualized in black by von Kossa stain. (**See Figures, Supplemental Digital Content 1 through 3,** http://links.lww.com/PRS/A964, http://links.lww.com/PRS/A965, and http://links.lww.com/PRS/A966, respectively.) (*Above* and *center, right*) Case 1: calcifications were localized only on the inside of the internal fibrous layer. (*Center, left*) Case 2: microcalcifications were observed even at the center of the wall (*black arrows*). (*Below*) Case 3: calcifications were stronger in the cyst wall than in the other cases.

become anti-inflammatory M2 macrophages with greater capacity for the induction of other mononuclear cells to produce angiogenic and fibrogenic cytokines, notably interleukin-4, interleukin-10, interleukin-13, and transforming growth factor-β1.[21] Thus, M2 macrophages are associated indirectly with angiogenesis and fibrogenesis. Our recent animal studies suggest that M2 macrophages are key players, contributing to fibrogenesis and calcification after fat grafting (unpublished data).

Three cases in this study had oil cysts from different periods after fat grafting: 2, 4, and 6 years. The oil cysts with a longer history appeared to show more calcification in the innermost layer

and a larger fibrous area adjacent to the degenerated fat portion than those with a shorter history, although our study included only a small number of cases. Calcified deposits were observed also in the intermediate fibrous area in the case with the longest history. These histopathologic findings and clinical computed tomographic images revealed that oil cysts, which are formed by 6 months and are filled with necrotized materials, are continuously inflammatory and calcifications continue to develop—very slowly—over time for several years; indeed, it seems that these progressive changes never end.

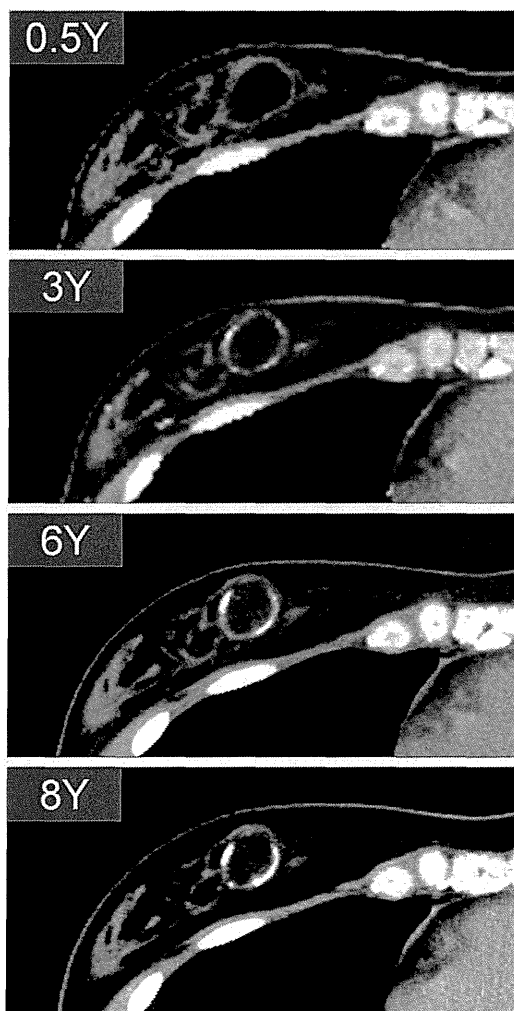We should never forget what has occurred as a result of immature techniques in the past and

Fig. 5. Sequential computed tomographic images of oil cysts taken from a patient (34-year-old woman) with multiple oil cysts in both breasts who did not undergo any removal of the cysts. The size of the oil cysts did not change between 3 and 8 years, but calcification progressed during that period. **(See also Figure, Supplemental Digital Content 5,** *http://links.lww.com/PRS/A968*.**)**

Fig. 6. Sequential mammographic images of a patient (30-year-old woman) who underwent fat grafting to the breast with no postoperative lumps. Calcifications were not apparent at 1 year (*left*), but sand-like macrocalcifications were clearly detected at 4 years (*center*) and 7 years (*right*). **(See Figure, Supplemental Digital Content 5,** *http://links.lww.com/PRS/A968*.**)**

but we should standardize and expand the use of this powerful and promising injectable with much greater care than was once used.

Kotaro Yoshimura, M.D.
Department of Plastic Surgery
University of Tokyo School of Medicine
7-3-1 Hongo, Bunkyo-Ku
Tokyo 113-8655, Japan
kotaro-yoshimura@umin.ac.jp

never repeat the history of prior fat grafting to the breast.[22] Large fat necrosis–inducing oil cysts must be avoided, although small fat necrosis resulting in sand-like calcification may be within acceptable limits. A bolus injection of fat always results in a large central necrosis and oil cysts. As recent technical advances have suggested,[4] we can prevent oil cysts by meticulously distributing fat tissue evenly and diffusely as tiny aliquots or noodles, paying great attention, using specific devices and techniques. We believe that sophisticated injection techniques are crucial for avoiding oil cysts among many surgeon-side factors affecting clinical outcomes. Adipose tissue and its stem/progenitor cells can volumize, vitalize, or harmonize pathologic tissues,
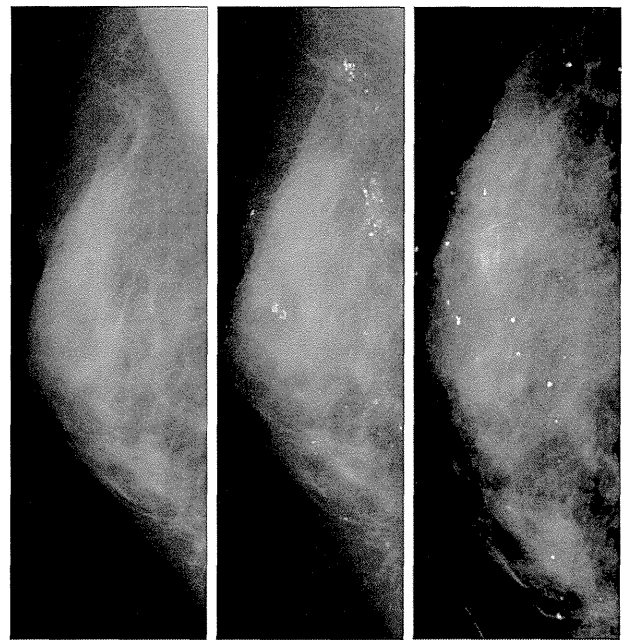
REFERENCES

1. Rigotti G, Marchi A, Galiè M, et al. Clinical treatment of radiotherapy tissue damage by lipoaspirate transplant: A healing process mediated by adipose-derived adult stem cells. *Plast Reconstr Surg.* 2007;119:1409–1422.
2. Coleman SR. Structural fat grafting: More than a permanent filler. *Plast Reconstr Surg.* 2006;118:108S–120S.
3. Matsumoto D, Sato K, Gonda K, et al. Cell-assisted lipotransfer: Supportive use of human adipose-derived cells for soft tissue augmentation with lipoinjection. *Tissue Eng.* 2006;12:3375–3382.
4. Coleman SR, Saboeiro AP. Fat grafting to the breast revisited: Safety and efficacy. *Plast Reconstr Surg.* 2007;119:775–785.
5. Illouz YG, Sterodimas A. Autologous fat transplantation to the breast: A personal technique with 25 years of experience. *Aesthetic Plast Surg.* 2009;33:706–715.
6. Yoshimura K, Sato K, Aoi N, et al. Cell-assisted lipotransfer for cosmetic breast augmentation: Supportive use of adipose-derived stem/stromal cells. *Aesthetic Plast Surg.* 2008;32:48–55.

7. Delay E, Garson S, Tousson G, Sinna R. Fat injection to the breast: Technique, results, and indications based on 880 procedures over 10 years. *Aesthet Surg J.* 2009;29:360–376.
8. Khouri RK, Eisenmann-Klein M, Cardoso E, et al. Brava and autologous fat transfer is a safe and effective breast augmentation alternative: Results of a 6-year, 81-patient, prospective multicenter study. *Plast Reconstr Surg.* 2012;129:1173–1187.
9. Kling RE, Mehrara BJ, Pusic AL, et al. Trends in autologous fat grafting to the breast: A national survey of the American Society of Plastic Surgeons. *Plast Reconstr Surg.* 2013;132:35–46.
10. Eto H, Kato H, Suga H, et al. The fate of adipocytes after non-vascularized fat grafting: Evidence of early death and replacement of adipocytes. *Plast Reconstr Surg.* 2012;129:1081–1092.
11. Suga H, Eto H, Aoi N, et al. Adipose tissue remodeling under ischemia: Death of adipocytes and activation of stem/progenitor cells. *Plast Reconstr Surg.* 2010;126:1911–1923.
12. Mu DL, Luan J, Mu L, Xin MQ. Breast augmentation by autologous fat injection grafting: Management and clinical analysis of complications. *Ann Plast Surg.* 2009;63:124–127.
13. Hyakusoku H, Ogawa R, Ono S, et al. Complications after autologous fat injection to the breast. *Plast Reconstr Surg.* 2009;123:360–370.
14. Wang CF, Zhou Z, Yan Y, et al. Clinical analysis of clustered microcalcifications after autologous fat injection for breast augmentation. *Plast Reconstr Surg.* 2011;127:1669–1673.
15. Rubin JP, Coon D, Zuley M, et al. Mammographic changes after fat transfer to the breast compared with changes after breast reduction: A blinded study. *Plast Reconstr Surg.* 2012;129:1029–1038.
16. Veber M, Tourasse C, Toussoun G, et al. Radiographic findings after breast augmentation by autologous fat transfer. *Plast Reconstr Surg.* 2011;127:1289–1299.
17. Zocchi ML, Zuliani F. Bicompartmental breast lipostructuring. *Aesthetic Plast Surg.* 2008;32:313–328.
18. Gosset J, Guerin N, Toussoun G, et al. Radiological evaluation after lipomodelling for correction of breast conservative treatment sequelae (in French). *Ann Chir Plast Esthet.* 2008;53:178–189.
19. Fairweather D, Cihakova D. Alternatively activated macrophages in infection and autoimmunity. *J Autoimmun.* 2009;33:222–230.
20. Martinez FO, Helming L, Gordon S. Alternative activation of macrophages: An immunologic functional perspective. *Annu Rev Immunol.* 2009;27:451–483.
21. Wick G, Grundtman C, Mayerl C, et al. The immunology of fibrosis. *Annu Rev Immunol.* 2013;31:107–135.
22. Report on autologous fat transplantation. ASPRS Ad-Hoc Committee on New Procedures, September 30, 1987. *Plast Surg Nurs.* 1987;7:140–141.

APPENDIX

See Figure, Supplemental Digital Content 1, which shows detailed data for the patient in case 1, a 24-year-old woman who underwent fat grafting for cosmetic breast augmentation 2 years earlier, *http://links.lww.com/PRS/A964.* She recognized hardness of the entirety of both breasts at 6 months and gradually recognized tenderness and abnormal sensations. She visited us for consultation. (*A*) She had well-projected breasts with tight skin. The contour of the upper pole appeared similar to a breast with implant contracture. (*B*) Preoperative

computed tomographic scan showed that there was a single large calcified oil cyst under each mammary gland. It was suspected that 100 to 200 ml of fat tissue had been introduced in a bolus injection before. (*C*) Removed oil cysts were filled with muddy content caused by fat necrosis. The oil cyst wall had innermost and outermost fibrous layers. (*D*) Hematoxylin and eosin staining showed that surfaces on both sides of the cyst wall were fibrosis layers. *Scale bar* = 300 μm. (*E*) Immunohistochemistry showed that there were regular and degenerated fatty portions between the inner and outer fibrous layers. *Scale bar* = 300 μm. (*F*) There were two types of fatty portions: a regular fatty portion and a degenerated fatty portion. The degenerated portion had many dead (perilipin-weak or -negative) adipocytes and fibrous areas. *Scale bar* = 100 μm. (*G*) The regular fatty portion showed round perilipin-positive adipocytes and lectin-positive vessels and capillaries. *Scale bar* = 50 μm. (*H*) The regular fatty portions had CD34+ adipose stem/progenitor cells around vessels and capillaries. *Scale bar* = 50 μm. (*I*) Von Kossa staining showed that calcifications were seen in the innermost fibrous layer. *Scale bars* = 500 and 300 μm.

See Figure, Supplemental Digital Content 2, which shows detailed data for the patient in case 2, a 30-year-old woman who underwent fat grafting for cosmetic breast augmentation 4 years earlier, *http://links.lww.com/PRS/A965.* She recognized multiple lumps in both breasts afterward. She wanted to have the lumps removed because of tenderness and contracture. (*A*) Her breasts had slightly projected upper poles, and multiple solid lumps were palpable. (*B*) Preoperative three-dimensional computed tomography clearly indicated two calcified large lumps below the mammary gland on each side. (*C*) The four removed lumps were of variable sizes. Calcified scales were seen on the inner surface of the cyst wall. (*D*) Immunohistology showed that large oil droplets (*arrows*) were seen in the degenerated fatty portion between the two surface fibrous layers. A regular fatty layer was rarely seen. *Scale bar* = 300 μm. (*E*) Degenerated portions showed many small and large oil droplets (perilipin-negative) in the fibrous area. All oil droplets were surrounded by MAC2+ macrophages. *Scale bars* = 300 and 100 μm. (*F*) Most of the macrophages were positive for both MAC2 and CD206, indicating that they were anti-inflammatory M2 macrophages. *Scale bar* = 30 μm. (*G*) Von Kossa staining showed that calcifications were seen not only in the innermost fibrous layer, but also in the intermediate fibrous area. *Scale bars* = 500, 100, and 60 μm.

See Figure, Supplemental Digital Content 3, which shows detailed data for the patient in case 3, a 30-year-old woman who underwent fat grafting for cosmetic breast augmentation 6 years earlier, http://links.lww.com/PRS/A966. She recognized multiple lumps in both breasts afterward. She wanted to have the lumps removed because of occasional pain. (A) Her left breast had an abnormal shape because of an underlying large lump. Other lumps were palpable, but their sizes were smaller. (B) Preoperative magnetic resonance imaging showed multiple oil cysts; the largest was located below the left mammary gland. (C) A large cyst had a very thick and calcified cyst wall and contained muddy, necrotic material inside. A smaller cyst had a thinner wall and scaly calcifications on the inner surface of the wall. (D) Hematoxylin and eosin staining showed degenerated fatty regions containing numerous oil droplets between the two fibrous surface layers. These oil drops had not been absorbed even after several years, suggesting that chronic inflammation in the cyst wall may be endless. No regular fatty portion was seen in this case with the longest history. Scale bar = 300 μm. (E) The fibrous area in the degenerated fatty portion showed many infiltrated macrophages around the oil droplets. Scale bars = 300 and 100 μm. (F) Von Kossa staining showed that the cyst wall of case 3 presented not only macrocalcifications on the inner surface, but also intense granular calcified deposits in the intermediate fibrous area, suggesting that long-term inflammation accompanied by M2 macrophages may induce calcifications. Scale bars = 300 μm, 1 mm, and 100 μm.

Plastic Surgery Level of Evidence Rating Scale—Therapeutic Studies

THERAPEUTIC

Level of Evidence	Qualifying Studies
I	Highest-quality, multicentered or single-centered, randomized controlled trial with adequate power; or systematic review of these studies
II	High-quality, randomized controlled trial; prospective cohort or comparative study; or systematic review of these studies
III	Retrospective cohort or comparative study; case-control study; or systematic review of these studies
IV	Case series with pre/post test; or only post test
V	Expert opinion developed via consensus process; case report or clinical example; or evidence based on physiology, bench research, or "first principles"

Find out more from the "Evidence-Based Medicine: How-to Articles" Collection at www.PRSJournal.com

ORIGINAL ARTICLE

Experimental

Application of Normobaric Hyperoxygenation to an Ischemic Flap and a Composite Skin Graft

Jun Araki
Harunosuke Kato
Kentaro Doi
Shinichiro Kuno
Kahori Kinoshita
Kazuhide Mineda
Koji Kanayama
Kotaro Yoshimura

Background: Hyperbaric oxygenation has been used for various purposes, but its clinical application is limited due to its pulmonary toxicity. We evaluated the therapeutic value of normobaric hyperoxygenation (NBO) for vascularized and nonvascularized tissue transplantation.
Methods: Tissue oxygen partial pressure (PtO_2) was measured for various organs in mice under inspiratory oxygen of 20%, 60%, or 100%. A rectangular skin flap (1×4 cm) or a composite skin graft (2×2 cm) was made on the back of mice, which were housed under 20% or 60% oxygen for the first 3 days after surgery. Cell survival was also examined in organ culture skin samples.
Results: PtO_2 varied among tissues/organs, but increased depending on inspiratory oxygen concentration in all tissues/organs. Although NBO with 100% O_2 was toxic, NBO with 60% O_2 was safe even when used continuously for a long period. NBO did not significantly improve survival of the rectangular skin flap. On the other hand, in the composite skin graft model, the engraftment area increased significantly (52 ± 10 at 20% vs 68 ± 5.1 at 60%) and contraction decreased significantly (42 ± 8.0 at 20% vs 27 ± 5.7 at 60%). Organ culture of a composite skin sample showed significant cell death under lower oxygen concentrations, supporting the data in vivo.
Conclusions: The composite graft was maintained until revascularization by plasmatic diffusion from surrounding tissues, in which PtO_2 was improved by NBO. NBO may be an effective adjunct therapy that can be performed readily after nonvascularized tissue grafting. (*Plast Reconstr Surg Glob Open* 2014;2:e152; doi: 10.1097/GOX.0000000000000029; Published online 15 May 2014.)

The concept of oxygen as a therapeutic agent was first introduced in the 1920s by Barach.[1] Since then, the effects of hypoxemia and its reversal with oxygen supplementation have been well-explored, leading to increased use of oxygenation for treating respiratory and/or cardiovascular insufficiency and postsurgery/postanesthesia conditions.[2–4] An extreme therapeutic example is hyperbaric oxygenation (HBO), which typically uses 100% oxygen at 3 atmospheres and has been applied for various purposes, including promoting wound healing for grafting or supporting flap survival.[5,6] HBO, however, can be used clinically only for 60–90 minutes per day due to its pulmonary toxicity.[7] The systemic influences of the strong toxicity and the repeated rebounding effects remain to be determined,

Supplemental digital content is available for this article. Clickable URL citations appear in the text.

and the therapeutic benefits of HBO remain controversial, limiting expanded use. The biological roles of oxygen in the skin and wound healing have been examined at the molecular level and its clinical usage were reviewed recently.[8,9]

In this study, we sought to develop a safer and more reliable hyperoxygenation method to improve tissue wound healing using normobaric hyperoxygenation (NBO). We first researched the effects of NBO with various fraction of inspiratory oxygen (FiO_2) on the tissue partial pressure of oxygen (PtO_2) in various tissues and organs. After establishing an optimized NBO protocol and confirming a beneficial effect on cell survival in skin organ culture, we examined the therapeutic value of postoperative NBO for improving clinical outcomes of an ischemic flap and a composite skin graft.

MATERIALS AND METHODS

Oxygen Pressure Measurement

All animal care was in accordance with institutional guidelines. Fifty-five Jcl:ICR mice (males, 7–10 weeks old) were purchased from the Nippon Bio-Supply Center (Tokyo, Japan). PtO_2 in mice ($n = 3$) was measured as described previously.[10] Briefly, it was measured with a modified Clark-type electrode (200 μm in diameter) and an oxygen monitor (Eiko Kagaku, Tokyo, Japan) under minimal anesthesia to prevent substantial cardiovascular or respiratory depression. The oxygen electrode was inserted directly into the abdominal subcutaneous tissue, the inguinal fat pad, the femoral muscles, the liver, and the kidney under oxygen at 20% (room air), 60%, or 100%. The sensor was placed in the tissue for at least 10 minutes until the measured value reaches a plateau. The partial pressures of oxygen in arterial blood (PaO_2) and venous blood (PvO_2) under oxygen at 20% (room air), 60%, or 100% were also measured with a blood gas analysis apparatus (ABL800 Flex, Radiometer, Tokyo, Japan).

Mice Models of a Skin Flap and a Composite Skin Graft

After a mouse was anesthetized, with an intraperitoneal injection of pentobarbital, 2 kinds of transplantation models were prepared.

A rectangular skin flap was used as a vascularized but partly ischemic tissue transplantation model, as described previously.[11] In this model, a cranial-based rectangular skin flap (1×4 cm; $n = 10$), including the subcutaneous tissue, was elevated on the back. After placing a thin synthetic film (Asahikasei, Tokyo, Japan) to prevent revascularization from the underlying wound bed, the skin flap was sutured orthotopically using 6-0 nylon.

A composite skin graft was used as a nonvascularized tissue transplantation model. In this model, a square-shaped composite skin (2×2 cm, $n = 10$) including the subcutaneous tissue was excised from the back and was immediately sutured orthotopically with 6-0 nylon, followed by a gauze dressing.

The animals of both models were divided into 2 groups, control and NBO. The control animals were housed under room air (20% oxygen), whereas NBO group animals were kept under NBO (normobaric 60% oxygen and 40% air) for the first 3 days after surgery and under room air for the remaining period. The animals were given free access to food and water. Experimental procedures are summarized in Figure 1 and Supplemental Figure S1. [See **Supplemental Digital Content** 1, which demonstrates animal models of a skin flap and a composite skin graft. (A) A quadrant skin flap was elevated on the back of mice and sutured to the original position. (B) A composite skin was excised on the back of mice and sutured to the original position. The tie-over dressing was performed and removed at 1 week, *http://links.lww.com/PRSGO/A31.*]

Measurement of Tissue Viability

Surgical sites were photographed at 1, 2, and 4 weeks after surgery. Areas of survival, contraction, and necrosis (or eschar formation) were measured. Each area was color-coded manually in yellow, white, and black (or gray) with graphics software (Photoshop CS6, Adobe Systems, San Jose, Calif.), followed by measuring the pixel number of each area.

Cell Viability in Skin Organ Culture

Small round skin fragments (6 mm in diameter) were harvested from the back of mice with a disposable punch biopsy (Kai Industries, Gifu, Japan). Skin samples were incubated in Dulbecco's modified Eagle medium containing 4% hyaluronate and 5% fetal bovine serum for 6 hours under 1% (hypoxia), 6% (normoxia), or 20% (hyperoxia) oxygen ($n = 3$ for each group). After washing with phosphate-buffered saline, they were incubated with Hoechst33342 (Dojindo, Kumamoto, Japan) and propidium iodide (PI; Sigma-Aldrich, St. Louis, Mo.) at 37°C for 30 minutes. The stained samples were evaluated under a TCS SP2 confocal microscope system (Leica, Heerbrugg, Switzerland). Ten serial images of the dermis were obtained at 3-μm intervals and were processed to produce a surface-rendered, 30-μm-thick, three-dimensional image. Numbers of all nuclei (Hoechst-positive) and dead nuclei (Hoechst- and PI-positive) were counted.
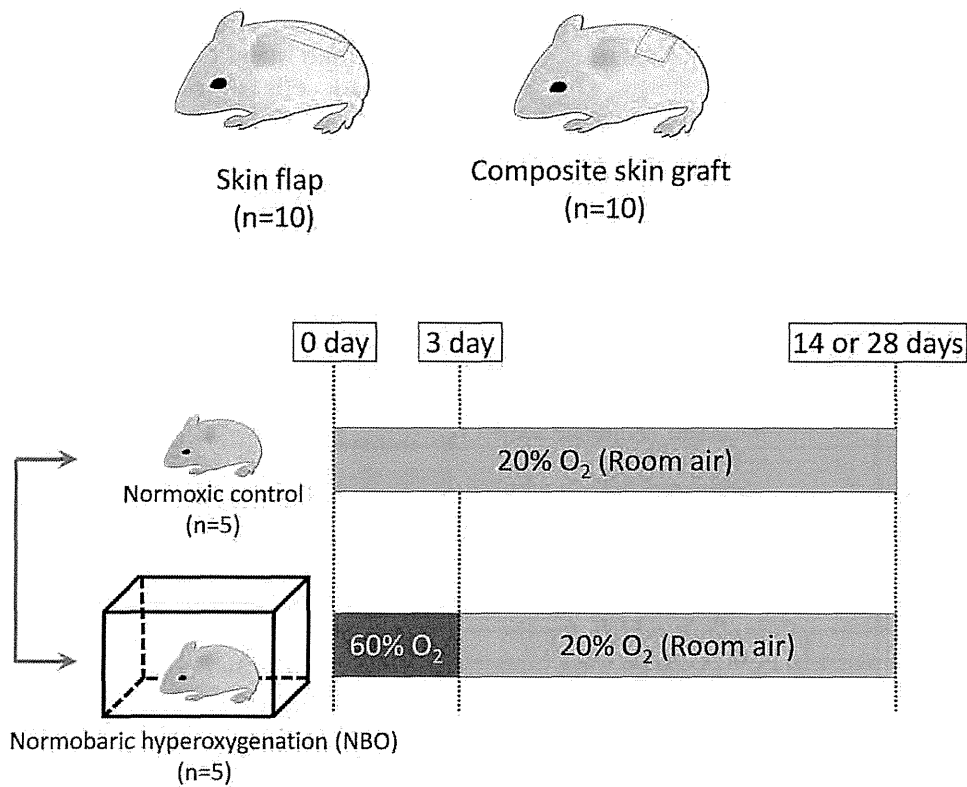
2

Fig. 1. Normoxic control and NBO application in mouse model of a rectangular skin flap and a composite skin graft. Using 20 ICR mice, a skin flap model ($n = 10$) and a composite skin graft model (a skin graft containing subcutaneous tissue; $n = 10$) were prepared (above) and divided into 2 groups: the normoxic control and NBO therapy groups (below). In the NBO group, normobaric hyperoxygenation with 60% O_2 was applied for the first 3 days after surgery.

Statistical Analysis

Results are described as means ± standard deviations. Comparisons between the 2 groups were performed using the unpaired Student's t test. Comparisons of more than 2 groups were made by analysis of variance with the Bonferroni correction. Statistical significance was defined as $P < 0.05$.

RESULTS

Oxygen Tension of Blood and Tissues Influenced by NBO

PaO_2 and PvO_2 measured in this study were 115 ± 27 mm Hg and 47 ± 10 mm Hg, suggesting that oxygen tension is very similar between mice and humans. It was also found that PtO_2 varied considerably among organs: PtO_2 (mm Hg) was 50 ± 9.3 in inguinal fat pad, 28 ± 14 in femoral muscle, 28 ± 16 in liver, 25 ± 16 in kidney, and 43 ± 9.5 in subcutaneous tissue (Fig. 2).

PaO_2 was increased to 217% and 250% by application of 60% (3 times that of room air) and 100% (5 times) oxygen, respectively, while PvO_2 was 134% (60% O_2) or 171% (100% O_2). NBO using high FiO_2 (60%

or 100% oxygen) increased PtO_2 in all organs/tissues tested, although the increase in PtO_2 was not proportional to the increase of FiO_2, as seen in PaO_2 and PvO_2. The increased percentage of PtO_2 under 60%/100% oxygen was 201%/475% in inguinal fat, 195%/484% in femoral muscle, 141%/259% in liver, 125%/136% in kidney, and 178%/290% in subcutaneous tissue, respectively (Fig. 2). These results supported previous studies showing PtO_2 of the skin and soft tissues.[12-14]

Treatment with normobaric 100% oxygen killed all mice in 2 days, although 100% oxygen at 2–3 atmospheres absolute is generally used in clinical HBO. We also found that long-term (several weeks) continuous application of normobaric 60% oxygen was not toxic and could be used as a continuous NBO therapy.

NBO Therapy for the Rectangular Skin Flap

The skin flap was evaluated at 1 week after surgery when the necrotic demarcation was definite. In the normoxic control group ($FiO_2 = 20\%$ for 7 days), skin flap areas of contraction, engraftment, and necrosis were 30% ± 4.3%, 18% ± 4.9%, and 51% ± 6.5% of the original flap size, respectively. On the
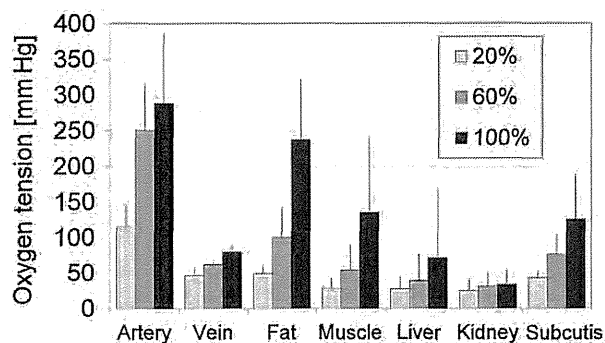
3

Fig. 2. Oxygen pressure of blood and organs under 3 different inspired oxygen concentrations. NBO (normobaric 60% or 100% oxygen) was applied to mice and compared with room air. PaO_2, PvO_2, and PtO_2 of all tested organs changed depending on the inspired oxygen concentrations, although the increase in PtO_2 was not always proportional to that of the inspired oxygen concentration.

other hand, in the NBO group (FiO_2 = 60% for the first 3 days and 20% for the next 4 days), flap areas of contraction, engraftment, and necrosis were 26% ± 6.6%, 20% ± 4.9%, and 54% ± 2.4% of the original flap size, respectively (Fig. 3). Normobaric 60% oxygenation therapy did not significantly improve the survival of the rectangle skin flap.

NBO Therapy for the Composite Skin Graft

The composite skin graft was evaluated at 2 and 4 weeks after surgery, but the eschar remained on the graft and disturbed precise evaluation of contraction, engraftment, and necrosis (Fig. 4A). Thus, we evaluated the composite skin graft only at 4 weeks by which time all eschars had disappeared and wound contraction was complete. In the control group (FiO_2 = 20% for 7 days), the areas of contraction, engraftment, and necrosis were 42% ± 8.0%, 52% ± 10%, and 6.1% ± 4.3% of the original graft size, respectively. In the NBO group (FiO_2 = 60% for the first 3 days and 20% for the next 25 days), the areas of contraction, engraftment, and necrosis were 27% ± 5.7%, 68% ± 5.2%, and 4.7% ± 3.1% of the original graft size, respectively (Fig. 4B). The 3-day NBO therapy significantly increased the engraftment area (P = 0.023) and decreased the contraction area (P = 0.014).

Organ-cultured Skin Viability under Hypoxia, Normoxia, and Hyperoxia

Skin samples were cultured in medium under 1% (8 mm Hg; hypoxia), 6% (46 mm Hg; normoxia), and 20% (152 mm Hg; hyperoxia) oxygen. As the PtO_2 of skin that we measured in mice was around 40–50 mm Hg, culture under 6% O_2 corresponded approximately with normoxic condition for the

skin sample in organ culture. Nuclei of dead cells were stained with PI, whereas all nuclei (both viable and dead cells) were stained with Hoechst33342 [Supplemental Fig. S2A, see **Supplemental Digital Content 2**, which demonstrates cell death assay for organ-cultured skin samples. (A) Skin samples were organ-cultured under various oxygen tensions: 1% (8 mm Hg; hypoxia), 6% (46 mm Hg; normoxia), and 20% (152 mm Hg; hyperoxia). All nuclei were stained with Hoechst33342 (blue), whereas nuclei of dead cells were stained also with PI (red). The control is a noncultured skin sample, *http://links. lww.com/PRSGO/A31*]. The number of dead cells in skin samples increased after organ culture. The proportion of dead cells was significantly higher under hypoxia than under normoxia or hyperoxia [Supplemental Fig. S2B, see **Supplemental Digital Content 2**, which demonstrates cell death assay for organ-cultured skin samples. (B) Dead cells increased significantly when cultured under hypoxic conditions, suggesting that PtO_2 of the surrounding recipient tissue may substantially affect the acute damage of the grafted tissue, *http://links. lww.com/PRSGO/A31*]. These results supported the in vivo results showing that nonvascularized tissue damage was affected by the oxygen tension of the microenvironment.

DISCUSSION

This study revealed that systemic NBO elevated PtO_2 in all tissues/organs and that 3-day postoperative NBO therapy using 60% oxygen improved engraftment significantly of a nonvascularized composite skin graft, but not of a vascularized skin flap. Tissues/organs with vascularization, such as a skin flap, a microsurgical free flap, and a transplanted kidney, are maintained by blood flow from the nutrient pedicles. On the other hand, tissues/organs without vascularization, such as a skin graft or fat graft, are maintained only by plasmatic diffusion from the surrounding vascularized tissue until revascularization occurs.

In our previous studies,[15–17] we found that the first 3 ischemic days are the critical period for determining whether the tissue will survive or die. Under severe ischemic or hypoxic (or even other stress) conditions, almost all differentiated functioning cells will die, but tissue-resident stem/progenitor cells can stay alive up to 3 days even without oxygen.[17] The resident stem/progenitor cells are even temporarily activated by tissue damage. If revascularization is achieved within the 3 days, the tissue may be partially repaired by activated and recruited stem/progenitor cells, but the tissue will finally necrotize in cases when the microenviron-
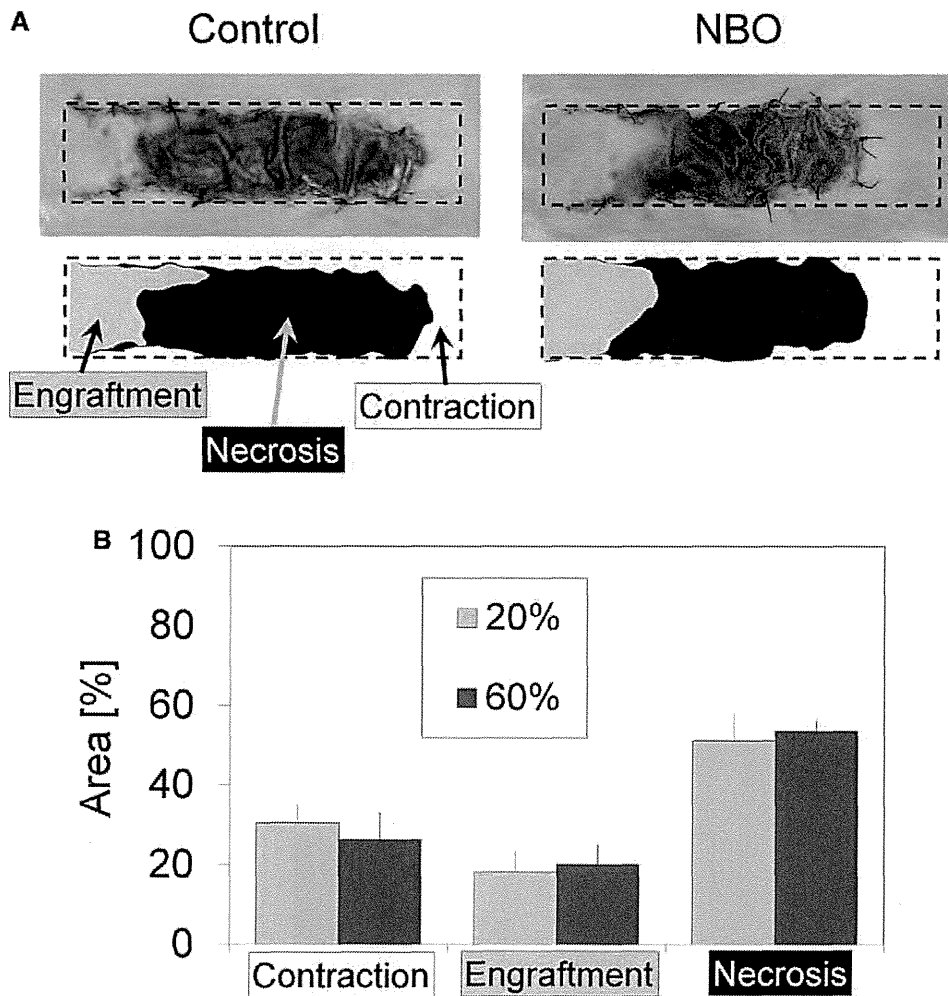
4

Fig. 3. NBO therapy for skin flap engraftment. A, NBO therapy using normobaric 60% oxygen was applied for the first 3 days after elevation of a skin flap and compared with the control at 1 week. The flap areas of contraction, engraftment, and necrosis were measured and are colored in white, yellow, and black, respectively. B, The areas of contraction, engraftment, and necrosis were not significantly different between the control and NBO groups.

ment does not improve within 3 days. This is the reason why we used NBO therapy only for the first 3 days in this study.

There are many reports on oxygen delivery to tissues/organs.[18,19,20] The oxygen content in a fluid (blood) of one deciliter $[C(O_2)]$ is expressed by the following equation[19,20]:

$$C(O_2)\left[(O_2)mL / (fluid)dL\right]$$
$$= P(O_2) \times 0.0225 + Hb \times S(O_2) \times 1.306,$$

where $P(O_2)$ is the mean oxygen partial pressure (15.4 kPa in arterial blood under 20% FiO_2), Hb is the hemoglobin concentration (g/dL), and $S(O_2)$ is the oxygen saturation (generally close to 1).

As indicated in this equation, hemoglobin in red blood cells usually contains most (~99%) of the ox-

ygen in blood, while the rest (the plasma portion) contains only about 1%. Under conditions where $S(O_2)$ is already about 1, applying hyperoxygenation with 60% O_2 will increase $P(O_2)$ (up to 3 times) alone and the increase in $C(O_2)$ is only up to 3%. Thus, this would suggest that the NBO does not provide much benefit to a vascularized flap. On the other hand, a nonvascularized skin fragment has no circulating blood and is maintained only by plasmatic diffusion from surrounding vascularized tissue. The oxygen content of the diffusing plasma, which does not contain hemoglobin, is proportional to $P(O_2)$, as indicated by the equation. Thus, it seems to be theoretically reasonable that increased $P(O_2)$ as a result of NBO will have a significant influence on the nonvascularized composite skin graft survival, but not on the elevated skin flap.
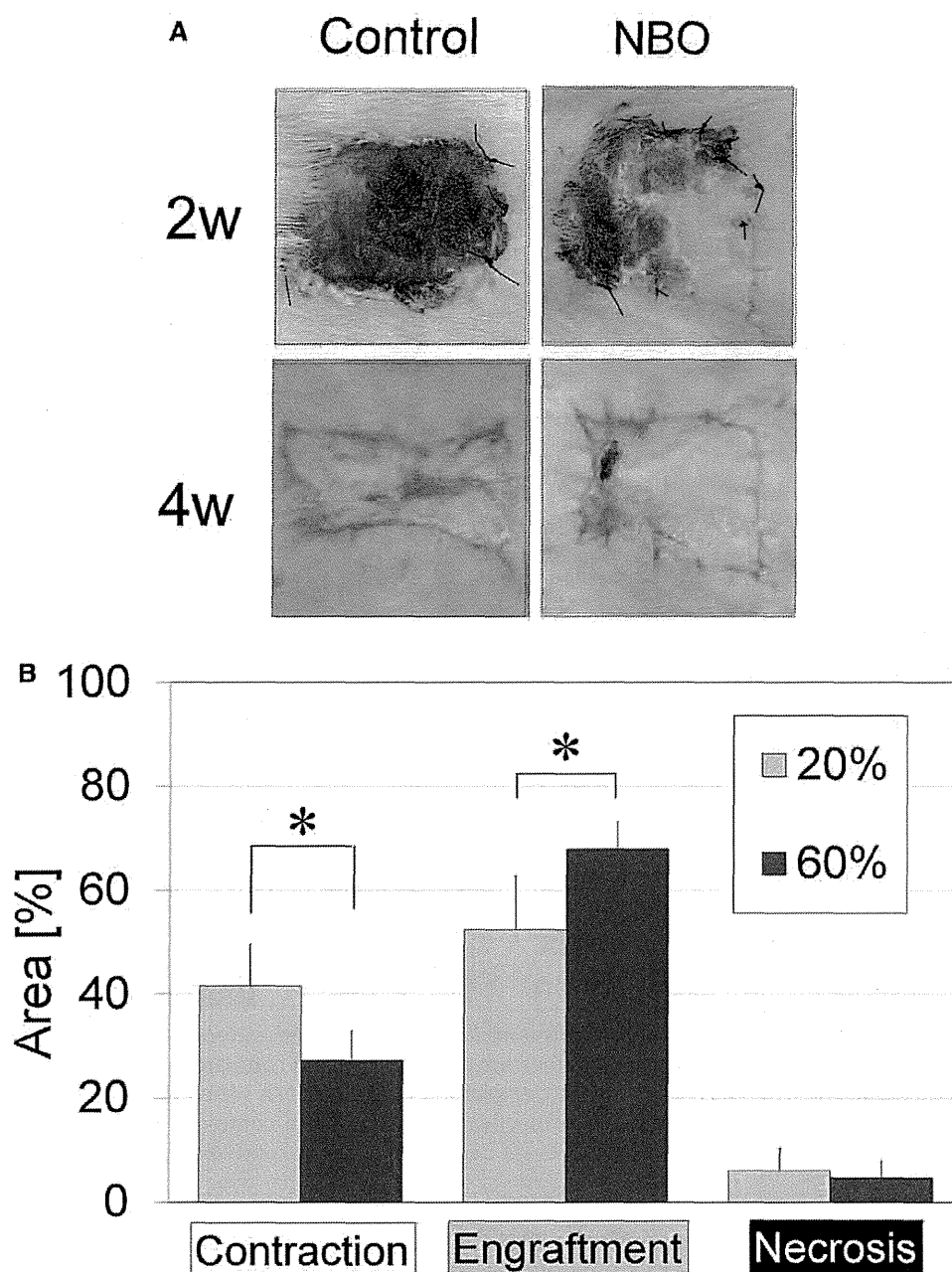
5

Fig. 4. NBO therapy for composite skin graft engraftment. A, NBO therapy using normobaric 60% oxygen was applied for the first 3 days after grafting of a composite skin and compared with the controls at 2 and 4 weeks. B, The areas of contraction, engraftment, and necrosis at 4 weeks were measured. The contraction area decreased significantly and the engraftment area increased significantly by NBO therapy.

Oxygen delivery to the tissues and wound was extensively studied by Hunt and Hopt and their colleagues. Their works cover a variety of physical factors and therapeutic modalities to influence with perfusion and tissue oxygen tension in relation to wound healing and postoperative infection in surgical patients.[12,14,21,22] Although there are a number of adjunct therapies for increasing the survival of vascularized flaps, including vasodilators, antioxidant drugs,[23] precursor mobilization,[24] hematopoiesis,[24,25] and cooling,[26] we have no reliable supportive treatments for nonvascularized tissue grafts. As shown in this study, systemic NBO therapy with 60% O_2 is a safe therapy and may bring significant benefits to graft survival through improving PtO_2 surrounding the recipient tissue. In clinical settings, systemic NBO therapy can be used readily with a simple oxygen mask or tent and may be a practical therapy to

6

boost engraftment of many kinds of nonvascularized tissue grafting. In addition, local NBO therapies may also be beneficial for closed wounds on which negative pressure wound therapy has no effect.[27] Although oxygen needs attention in terms of handling,[7,28] it may be useful in diverse ways in the field of plastic surgery.

Kotaro Yoshimura, MD
Department of Plastic Surgery
University of Tokyo
7-3-1 Hongo, Bunkyo-Ku
Tokyo 113–8655, Japan
E-mail: kotaro-yoshimura@umin.ac.jp

ACKNOWLEDGMENTS

REFERENCES

1. Barach AL. The therapeutic use of oxygen. *JAMA* 1922;79:693–698.
2. Hayes MA, Timmins AC, Yau EH, et al. Elevation of systemic oxygen delivery in the treatment of critically ill patients. *N Engl J Med.* 1994;330:1717–1722.
3. Tarpy SP, Celli BR. Long-term oxygen therapy. *N Engl J Med.* 1995;333:710–714.
4. Greif R, Akça O, Horn EP, et al.; Outcomes Research Group. Supplemental perioperative oxygen to reduce the incidence of surgical-wound infection. *N Engl J Med.* 2000;342:161–167.
5. Perrins DJ. Influence of hyperbaric oxygen on the survival of split skin grafts. *Lancet* 1967;1:868–871.
6. Friedman HI, Fitzmaurice M, Lefaivre JF, et al. An evidence-based appraisal of the use of hyperbaric oxygen on flaps and grafts. *Plast Reconstr Surg.* 2006;117:175S–190S.
7. Deneke SM, Fanburg BL. Normobaric oxygen toxicity of the lung. *N Engl J Med.* 1980;303:76–86.
8. Semenza GL. O2 sensing: only skin deep? *Cell* 2008;133:206–208.
9. Sen CK. Wound healing essentials: let there be oxygen. *Wound Repair Regen.* 2009;17:1–18.
10. Eto H, Suga H, Inoue K, et al. Adipose injury-associated factors mitigate hypoxia in ischemic tissues through activation of adipose-derived stem/progenitor/stromal cells and induction of angiogenesis. *Am J Pathol.* 2011;178:2322–2332.
11. Ceradini DJ, Kulkarni AR, Callaghan MJ, et al. Progenitor cell trafficking is regulated by hypoxic gradients through HIF-1 induction of SDF-1. *Nat Med.* 2004;10:858–864.
12. LaVan FB, Hunt TK. Oxygen and wound healing. *Clin Plast Surg.* 1990;17:463–472.
13. Clavijo-Alvarez JA, Sims CA, Pinsky MR, et al. Monitoring skeletal muscle and subcutaneous tissue acid-base status and oxygenation during hemorrhagic shock and resuscitation. *Shock* 2005;24:270–275.
14. Ueno C, Hunt TK, Hopf HW. Using physiology to improve surgical wound outcomes. *Plast Reconstr Surg.* 2006;117(7 Suppl):59S–71S.
15. Suga H, Eto H, Aoi N, et al. Adipose tissue remodeling under ischemia: death of adipocytes and activation of stem/progenitor cells. *Plast Reconstr Surg.* 2010;126:1911–1923.
16. Yoshimura K, Eto H, Kato H, et al. In vivo manipulation of stem cells for adipose tissue repair/reconstruction. *Regen Med.* 2011;6(6 Suppl):33–41.
17. Eto H, Kato H, Suga H, et al. The fate of adipocytes after nonvascularized fat grafting: evidence of early death and replacement of adipocytes. *Plast Reconstr Surg.* 2012;129:1081–1092.
18. Guo-Qian Y, Gang W, Zhi-Yong S. Investigation on the microcirculation effect of local application of natural hirudin on porcine random skin flap venous congestion. *Cell Biochem Biophys.* 2012;62:141–146.
19. Thomas D. The physiology of oxygen delivery. *Vox Sang.* 2004;87:70–73.
20. Lumb AB, Nair S. Effects of increased inspired oxygen concentration on tissue oxygenation: theoretical considerations. *Eur J Anaesthesiol.* 2010;27:275–279.
21. Hunt TK, Linsey M, Grislis H, et al. The effect of differing ambient oxygen tensions on wound infection. *Ann Surg.* 1975;181:35–39.
22. Chang N, Goodson WH III, Gottrup F, et al. Direct measurement of wound and tissue oxygen tension in postoperative patients. *Ann Surg.* 1983;197:470–478.
23. Bächle AC, Mörsdorf P, Rezaeian F, et al. N-acetylcysteine attenuates leukocytic inflammation and microvascular perfusion failure in critically ischemic random pattern flaps. *Microvasc Res.* 2011;82:28–34.
24. Harder Y, Amon M, Schramm R, et al. Erythropoietin reduces necrosis in critically ischemic myocutaneous tissue by protecting nutritive perfusion in a dose-dependent manner. *Surgery* 2009;145:372–383.
25. Plock JA, Tromp AE, Contaldo C, et al. Hemoglobin vesicles reduce hypoxia-related inflammation in critically ischemic hamster flap tissue. *Crit Care Med.* 2007;35:899–905.
26. Kubulus D, Amon M, Roesken F, et al. Experimental cooling-induced preconditioning attenuates skin flap failure. *Br J Surg.* 2005;92:1432–1438.
27. Masden D, Goldstein J, Endara M, et al. Negative pressure wound therapy for at-risk surgical closures in patients with multiple comorbidities: a prospective randomized controlled study. *Ann Surg.* 2012;255:1043–1047.
28. Winslow RM. Oxygen: the poison is in the dose. *Transfusion* 2013;53:424–437.

7

Tenofovir alafenamide versus tenofovir disoproxil fumarate, coformulated with elvitegravir, cobicistat, and emtricitabine, for initial treatment of HIV-1 infection: two randomised, double-blind, phase 3, non-inferiority trials

Paul E Sax, David Wohl, Michael T Yin, Frank Post, Edwin DeJesus, Michael Saag, Anton Pozniak, Melanie Thompson, Daniel Podzamczer,
Jean Michel Molina, Shinichi Oka, Ellen Koenig, Benoit Trottier, Jaime Andrade-Villanueva, Gordon Crofoot, Joseph M Custodio,
Andrew Plummer, Lijie Zhong, Huyen Cao, Hal Martin, Christian Callebaut, Andrew K Cheng, Marshall W Fordyce, Scott McCallister, for the
GS-US-292-0104/0111 Study Team*

Summary

Background Tenofovir disoproxil fumarate can cause renal and bone toxic effects related to high plasma tenofovir concentrations. Tenofovir alafenamide is a novel tenofovir prodrug with a 90% reduction in plasma tenofovir concentrations. Tenofovir alafenamide-containing regimens can have improved renal and bone safety compared with tenofovir disoproxil fumarate-containing regimens.

Methods In these two controlled, double-blind phase 3 studies, we recruited treatment-naive HIV-infected patients with an estimated creatinine clearance of 50 mL per min or higher from 178 outpatient centres in 16 countries. Patients were randomly assigned (1:1) to receive once-daily oral tablets containing 150 mg elvitegravir, 150 mg cobicistat, 200 mg emtricitabine, and 10 mg tenofovir alafenamide (E/C/F/tenofovir alafenamide) or 300 mg tenofovir disoproxil fumarate (E/C/F/tenofovir disoproxil fumarate) with matching placebo. Randomisation was done by a computer-generated allocation sequence (block size 4) and was stratified by HIV-1 RNA, CD4 count, and region (USA or ex-USA). Investigators, patients, study staff, and those assessing outcomes were masked to treatment group. All participants who received one dose of study drug were included in the primary intention-to-treat efficacy and safety analyses. The main outcomes were the proportion of patients with plasma HIV-1 RNA less than 50 copies per mL at week 48 as defined by the the US Food and Drug Adminstration (FDA) snapshot algorithm (pre-specified non-inferiority margin of 12%) and pre-specified renal and bone endpoints at 48 weeks. These studies are registered with ClinicalTrials.gov, numbers NCT01780506 and NCT01797445.

Findings We recruited patients from Jan 22, 2013, to Nov 4, 2013 (2175 screened and 1744 randomly assigned), and gave treatment to 1733 patients (866 given E/C/F/tenofovir alafenamide and 867 given E/C/F/tenofovir disoproxil fumarate). E/C/F/tenofovir alafenamide was non-inferior to E/C/F/tenofovir disoproxil fumarate, with 800 (92%) of 866 patients in the tenofovir alafenamide group and 784 (90%) of 867 patients in the tenofovir disoproxil fumarate group having plasma HIV-1 RNA less than 50 copies per mL (adjusted difference 2·0%, 95% CI −0·7 to 4·7). Patients given E/C/F/tenofovir alafenamide had significantly smaller mean serum creatinine increases than those given E/C/F/tenofovir disoproxil fumarate (0·08 vs 0·12 mg/dL; p<0·0001), significantly less proteinuria (median % change −3 vs 20; p<0·0001), and a significantly smaller decrease in bone mineral density at spine (mean % change −1·30 vs −2·86; p<0·0001) and hip (−0·66 vs −2·95; p<0·0001) at 48 weeks.

Interpretation Through 48 weeks, more than 90% of patients given E/C/F/tenofovir alafenamide or E/C/F/tenofovir disoproxil fumarate had virological success. Renal and bone effects were significantly reduced in patients given E/C/F/tenofovir alafenamide. Although these studies do not have the power to assess clinical safety events such as renal failure and fractures, our data suggest that E/C/F/tenofovir alafenamide will have a favourable long-term renal and bone safety profile.

Funding Gilead Sciences.

Introduction

Guidelines for initial treatment of HIV-1 infection recommend the use of two nucleoside reverse transcriptase inhibitors plus a third active drug from a different class.[1] Of nucleoside reverse transcriptase inhibitors, tenofovir disoproxil fumarate is included in most recommended regimens. Although potent and generally well tolerated, tenofovir disoproxil fumarate can cause clinically significant renal toxic effects,[2] especially in patients with risk factors for kidney disease or who are receiving concomitant ritonavir-boosted protease inhibitors.[3,4] Additionally, tenofovir disoproxil fumarate has been associated with greater reductions in bone mineral density than other antiretroviral drugs.[5] In one observational study,[6]

Republic (E Koenig MD);
Clinique Medicale L'Actuale in
Montreal, Montreal, Canada
(B Trottier MD); Unidad de VIH
del Hospital Civil de
Guadalajara, CUCS, U de G
Guadalajara, Mexico
(J Andrade-Villanueva MD);
Gordon Crofoot Research,
Houston, TX, USA
(G Crofoot MD); and Gilead
Sciences, Foster City, CA, USA
(J M Custodio PharmD,
A Plummer MS, L Zhong PhD,
H Cao MD, H Martin MD,
C Callebaut PhD, A K Cheng MD,
M W Fordyce MD,
S McCallister MD)

Correspondence to:
Dr Paul E Sax, Division of
Infectious Diseases and
Department of Medicine,
Brigham and Women's Hospital,
and Harvard Medical School,
Boston, MA 02115, USA
psax@partners.org

Research in context

Evidence before this study

Although potent and generally well tolerated, tenofovir disoproxil fumarate might lead to clinically significant renal and bone disease. The risk of these side-effects is related to plasma concentrations of tenofovir. The novel tenofovir prodrug tenofovir alafenamide delivers 90% lower plasma tenofovir compared with standard tenofovir disoproxil fumarate. This pharmacology might reduce the off-target effects of tenofovir, in particular renal and bone toxicity. A phase 2 comparative trial of tenofovir alafenamide versus tenofovir disoproxil fumarate (both coformulated with elvitegravir, cobicistat, and emtricitabine [E/C/F]) showed similar efficacy of tenofovir alafenamide and tenofovir disoproxil fumarate with a significantly reduced effect on estimated glomerular filtration rate, tubular proteinuria, and bone mineral density. We did a systematic search of PubMed to explore the use of tenofovir alafenamide in treatment-naive patients, with a particular focus on renal and bone safety in treatment-naive patients. Search terms included "tenofovir alafenamide" AND "naive" AND "renal" OR "bone." Searches were limited to articles published in English between 1997 and March, 2015. Only one article was retrieved, which was the phase 2 randomised clinical trial comparing E/C/F/tenofovir alafenamide with E/C/F/tenofovir disoproxil fumarate.

Added value of this study

These two fully-powered phase 3 double-blind, international clinical trials compared single-tablet regimens of E/C/F/tenofovir alafenamide with E/C/F/tenofovir disoproxil fumarate, with results confirming the earlier findings. Both regimens showed higher than 90% efficacy, with low (<1%) rates of discontinuations due to adverse events. Compared with tenofovir disoproxil fumarate, tenofovir alafenamide treatment led to smaller decreases in estimated glomerular filtration rate, less proteinuria (significant for all types measured), and had a more favourable effect on hip and spine bone mineral density. All lipid fractions increased more in the tenofovir alafenamide than in the tenofovir disoproxil fumarate group with similar total to HDL cholesterol ratios.

Implications of all the available evidence

E/C/F/tenofovir alafenamide is a highly effective regimen for treatment-naive patients, with more favourable effects than E/C/F/tenofovir disoproxil fumarate on renal and bone health. The hope is that these findings will translate into improved safety of tenofovir alafenamide-based antiretroviral therapy over years of treatment while maintaining a similarly high efficacy rate.

investigators noted that tenofovir disoproxil fumarate exposure was associated with an increased rate of fractures.

As a prodrug, tenofovir disoproxil fumarate is initially metabolised to tenofovir, which is subsequently metabolised in cells to tenofovir-diphosphate. Although intracellular tenofovir-diphosphate is responsible for the drug's antiviral activity, higher circulating plasma levels of tenofovir have been associated with an increased risk of both renal and bone toxicity.[7–10] A novel tenofovir prodrug tenofovir alafenamide results in roughly four times higher intracellular concentrations of the active metabolite tenofovir-diphosphate compared with tenofovir disoproxil fumarate, allowing for much lower doses of tenofovir alafenamide versus tenofovir disoproxil fumarate.[11] Because of tenofovir alafenamide's reduced dose and the improved stability, plasma exposure of tenofovir is 90% lower with tenofovir alafenamide than with tenofovir disoproxil fumarate, which is believed to reduce the risk of renal and bone toxicity.[7]

Findings of a phase 2 comparative trial[12] of tenofovir alafenamide versus tenofovir disoproxil fumarate (both coformulated with elvitegravir, cobicistat, and emtricitabine) showed similar antiviral activity of tenofovir alafenamide and tenofovir disoproxil fumarate, with a significantly reduced effect of tenofovir alafenamide compared to tenofovir disoproxil fumarate on estimated glomerular filtration rate, tubular proteinuria, and bone mineral density. To confirm these findings, we did two phase 3, double-blind clinical trials comparing elvitegravir, cobicistat, emtricitabine, and tenofovir

alafenamide (E/C/F/tenofovir alafenamide) with elvitegravir, cobicistat, emtricitabine, and tenofovir disoproxil fumarate (E/C/F/tenofovir disoproxil fumarate), with a protocol-specified focus on renal and bone safety.

Methods

Study design and patients

GS-US-292-0104 and GS-US-292-0111 are randomised, double-blind, multicentre, active-controlled phase 3 trials done at 134 sites in North America, Europe, Australia, Japan, and Thailand (GS-US-292-0104), and 128 sites in North America, Europe, and Latin America (GS-US-292-0111). Studies were undertaken in accordance with the Declaration of Helsinki and were approved by central or site-specific review boards or ethics committees. All patients gave written informed consent. Adults (aged ≥18 years) were enrolled if they had HIV-1 and no previous antiretroviral treatment, had HIV-1 RNA concentration of at least 1000 copies per mL, and an estimated glomerular filtration (creatinine clearance, Cockcroft-Gault) rate of at least 50 mL per min. Eligible patients had a screening HIV-1 genotype showing sensitivity to elvitegravir, emtricitabine, and tenofovir. No CD4 entry criteria were used. We excluded patients with positive hepatitis B surface antigen or hepatitis C antibody or a new AIDS-defining illness within 30 days of screening.

Randomisation and masking

Eligible patients were randomly assigned (1:1) to receive either coformulated 150 mg elvitegravir, 150 mg cobicistat,

200 mg emtricitabine, and 10 mg tenofovir alafenamide once a day, or coformulated 150 mg elvitegravir, 150 mg cobicistat, 200 mg emtricitabine, and 300 mg tenofovir disoproxil fumarate once a day. Both regimens were given with food. Patients also received placebo tablets matching the alternative treatment; thus, investigators, patients, and study staff giving treatment, assessing outcomes, and collecting data were masked to treatment group. A computer-generated allocation sequence (block size 4) was created by Bracket (San Francisco, CA, USA), and randomisation was stratified by HIV-1 RNA ($\leq$100000 copies per mL, >100000 to $\leq$400000 copies per mL, or >400000 copies per mL), CD4 count (<50 cells per μL, 50–199 cells per μL, or $\geq$200 cells per μL), and region (USA or ex-USA) at screening. Study investigators determined eligibility, obtained a participant number, and received automated treatment assignment based on a randomisation sequence.

Procedures
Post-baseline study visits occurred at weeks 2, 4, 8, 12, 16, 24, 36, and 48, after which patients continued masked treatment with visits every 12 weeks until week 96. After the primary endpoint had been reached, masked treatment with study drug was extended to week 144. Laboratory tests included haematological analysis, serum chemistry tests, fasting lipid parameters, CD4 counts, measures of renal function (estimated glomerular filtration rate, urine protein to creatinine ratio, urine albumin to creatinine ratio, retinol binding protein to creatinine ratio, β2-microglobulin to creatinine ratio, fractional excretion of uric acid, and fractional excretion of phosphate; Covance Laboratories, Indianapolis, IN, USA), and measurement of HIV RNA concentration (Roche TaqMan 2.0; Roche Diagnostics, Rotkreuz, Switzerland).

We used definitions of suboptimum virological response (<1 $\log_{10}$ reduction from baseline HIV-1 RNA and $\geq$50 copies per mL at the week 8 visit, confirmed at a subsequent visit) and virological rebound (plasma HIV-1 RNA <50 copies per mL, then having HIV-1 RNA $\geq$50 copies per mL, confirmed at a subsequent visit) to assess virological response. We defined virological failure as plasma HIV-1 RNA greater than or equal to 50 copies per mL and less than 1 $\log_{10}$ reduction from baseline at week 8, or 50 copies per mL or more HIV-1 RNA after previous suppression to less than 50 copies per mL or more than a 1 $\log_{10}$ increase in HIV-1 RNA from nadir. Any participant meeting these criteria had a second, confirmatory sample drawn within 3–6 weeks. Confirmatory samples with 400 copies per mL or more HIV-1 RNA were sent for HIV-1 genotype and phenotype analysis (PhenoSenseGT for Protease and Reverse Transcriptase genes, GenSeq Integrase and Phenosense Integrase for the Integrase gene; Monogram Biosciences, South San Francisco, CA, USA).

In all patients, dual energy x-ray absorptiometry scans of the lumbar spine and hip were done at baseline, week 24, and week 48 to measure percent changes in bone mineral density. The scans were processed by BioClinica (Newton, PA, USA). The preliminary results were reviewed twice by an independent data monitoring committee when half of patients had completed week 12 and when all patients had completed week 24 of follow-up, respectively. The primary endpoint analysis was done after all enrolled patients had completed their week 48 study visit or had prematurely discontinued study drug.

The primary endpoint was the proportion of patients who had plasma HIV-1 RNA less than 50 copies per mL at week 48 as defined by the the US Food and Drug Adminstration (FDA) snapshot algorithm.[13] Four key safety endpoints were pre-specified with multiplicity adjustments: hip bone mineral density, spine bone mineral density, serum creatinine, and treatment-emergent proteinuria. Additional secondary endpoints included treatment responses by subgroups, proportion of patients with plasma HIV-1 RNA less than 50 copies per mL when classifying missing as failure and missing as excluded, patients with HIV-1 RNA less than 20 copies per mL by snapshot, and change in CD4 count from baseline.

Statistical analysis
These two phase 3 studies were combined for a pre-specified pooled efficacy and safety analysis. Within each phase 3 study, for each of two interim analyses done for the independent data monitoring committee meeting, an α of 0·00001 was spent. Therefore, the significance level for the 1-sided non-inferiority test in the primary analysis at week 48 was 0·02499, equivalent to a two-sided 95·002% CI. The percentage differences and the associated 95·002% CIs were computed with the baseline HIV-1 RNA concentration and region stratum adjusted Mantel-Haenszel proportions.[14] To control for the overall type I error in the assessment of the primary efficacy endpoint and the four key safety endpoints, hypothesis testing was done in sequential order. The primary hypothesis of non-inferiority of E/C/F/tenofovir alafenamide relative to E/C/F/tenofovir disoproxil fumarate, with respect to the proportion of patients with less than 50 copies per mL of HIV-1 RNA at week 48 (as defined by the FDA snapshot algorithm) was tested first. The non-inferiority test was done at a one-sided, 0·02499 α level. If noninferiority was established, multiplicity adjustments were undertaken for the following safety endpoints with a fallback procedure[15] in the sequential order given below with prespecified two-sided α levels: hip bone mineral density (α=0·02), spine bone mineral density (α=0·01), serum creatinine (α=0·01998), and treatment-emergent proteinuria (α=0·00). The adjusted α levels were dependent on the results from preceding tests. For all the four safety endpoints, two-sided superiority tests were done.
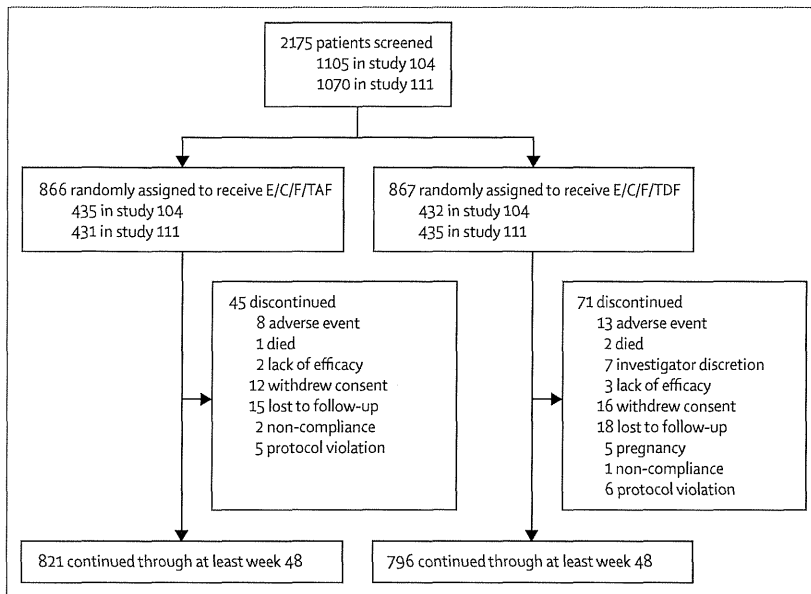
Figure 1: Trial profile
E/C/F/TAF=elvitegravir, cobicistat, emtricitabine, tenofovir alafenamide. E/C/F/TDF=elvitegravir, cobicistat, emtricitabine, tenofovir disoproxil fumarate.

	Elvitegravir, cobicistat, emtricitabine, tenofovir alafenamide (n=866)	Elvitegravir, cobicistat, emtricitabine, tenofovir disoproxil fumarate (n=867)
Age (years)	33 (26–42)	35 (28–44)
Women	133 (15%)	127 (15%)
Ethnic origin		
White	485 (56%)	498 (57%)
Black or African heritage	223 (26%)	213 (25%)
Hispanic or Latino	167 (19%)	167 (19%)
Asian	91 (11%)	89 (10%)
HIV disease status		
Asymptomatic	780 (90%)	802 (93%)
Symptomatic	53 (6%)	35 (4%)
AIDS	30 (4%)	26 (3%)
HIV risk factor		
Heterosexual sex	210 (24%)	219 (25%)
Homosexual sex§	652 (75%)	645 (74%)
Intravenous drug use	5 (1%)	6 (1%)
Median HIV-1 RNA ($\log_{10}$ c/mL)	4·58 (4·04–4·95)	4·58 (4·15–4·96)
HIV-1 RNA concentration >100 000 copies per mL	196 (23%)	195 (22%)
Median CD4 count (cells per μL)	404 (283–550)	406 (291–542)
Number with CD4 cell count (cells per μL)		
<50	24 (3%)	27 (3%)
≥50 to <200	88 (10%)	90 (10%)
≥200	753 (87%)	750 (87%)
Median estimated glomerular filtration rate (Cockcroft-Gault; mL/min)	117 (100–136)	114 (99–134)
Median BMI (kg/m²)	24·4 (22·0–28·0)	24·5 (21·7–28·0)

Data are median (IQR) or n (%).

Table 1: Baseline characteristics

For pooled data, assessment of non-inferiority of E/C/F/tenofovir alafenamide compared with E/C/F/tenofovir disoproxil fumarate was done with a two-sided 95% CI (α level not adjusted), with a prespecified non-inferiority margin of 12%. In the snapshot analysis using full analysis set that included all participants randomly assigned and receiving at least one dose of study drug, participants with less than 50 copies per mL of HIV-1 RNA between days 294 and 377 (week 48 window) were classified as successes. Participants with missing HIV-1 RNA data for the week 48 analysis window, who discontinued study drug, or who changed treatment before week 48 were classified as failures. A sample size of 840 patients in each study provided at least 95% power to establish non-inferiority between the two treatment groups with an overall response rate of 85% for viral suppression at week 48. Sample sizes were calculated with nQuery Advisor (version 6.0).

We did a prespecified, per-protocol snapshot analysis, which included all participants who enrolled, received at least one dose of study drug, and did not meet any of the following prespecified criteria: discontinuation of study drug before week 48 or HIV RNA data missing in week 48 analysis window, and adherence in the bottom 2·5th percentile.

Change from baseline in CD4 cell count at week 48 was summarised by treatment group with descriptive statistics based on recorded, on-treatment data in the full analysis set. The differences in changes from baseline in CD4 cell count between treatment groups and the 95% CI were constructed with analysis of variance model, including baseline HIV-1 RNA and region as fixed covariates in the model.

The safety population included all randomly assigned patients who received at least one dose of study drug. All safety data are described in summary form on all data collected after the date study drug was first given and up to 30 days after the last dose of study drug, if the participant discontinued treatment. Adherence to the investigational antiretroviral regimens was computed as number of pills taken divided by number of pills prescribed. Adverse events were coded with the Medical Dictionary for Regulatory Activities (version 17.0). We used Fisher's exact test to compare treatment differences for adverse events and Wilcoxon rank sum test to compare treatment differences for continuous laboratory test results (SAS; version 9.2).

These studies were done according to protocol without significant deviations and are registered with ClinicalTrials.gov, numbers NCT01780506 and NCT01797445.

Outcomes

The main outcomes were the proportion of patients with plasma HIV-1 RNA less than 50 copies per mL (non-inferiority margin of 12%) and pre-specified renal and bone endpoints at 48 weeks (centrally assessed). Secondary outcomes were percentage change from

baseline in hip bone mineral density at week 48, percentage change from baseline in spine bone mineral density at week 48, change from baseline in serum creatinine at week 48, treatment-emergent proteinuria through week 48, proportion of participants with HIV-1 RNA lower than 20 per mL at week 48, change from baseline in CD4 cell count at week 48, percentage change from baseline in urine retinol binding protein to creatinine ratio at week 48, percentage change from baseline in urine β2-microglobulin to creatinine ratio at week 48, percentage change from baseline in urine

protein to creatinine ratio at week 48, and percentage change from baseline in urine albumin to creatinine ratio. Safety was assessed by physical examinations, laboratory tests, 12-lead electrocardiogram, and recording of adverse events. The pharmacokinetics of tenofovir alafenamide and its metabolite, tenofovir was assessed through an intensive pharmacokinetic substudy done on a non-randomised subset of patients at week 4 or 8, which included plasma sampling for tenofovir alafenamide and tenofovir and peripheral blood mononuclear cell sampling for intracellular tenofovir-diphosphate
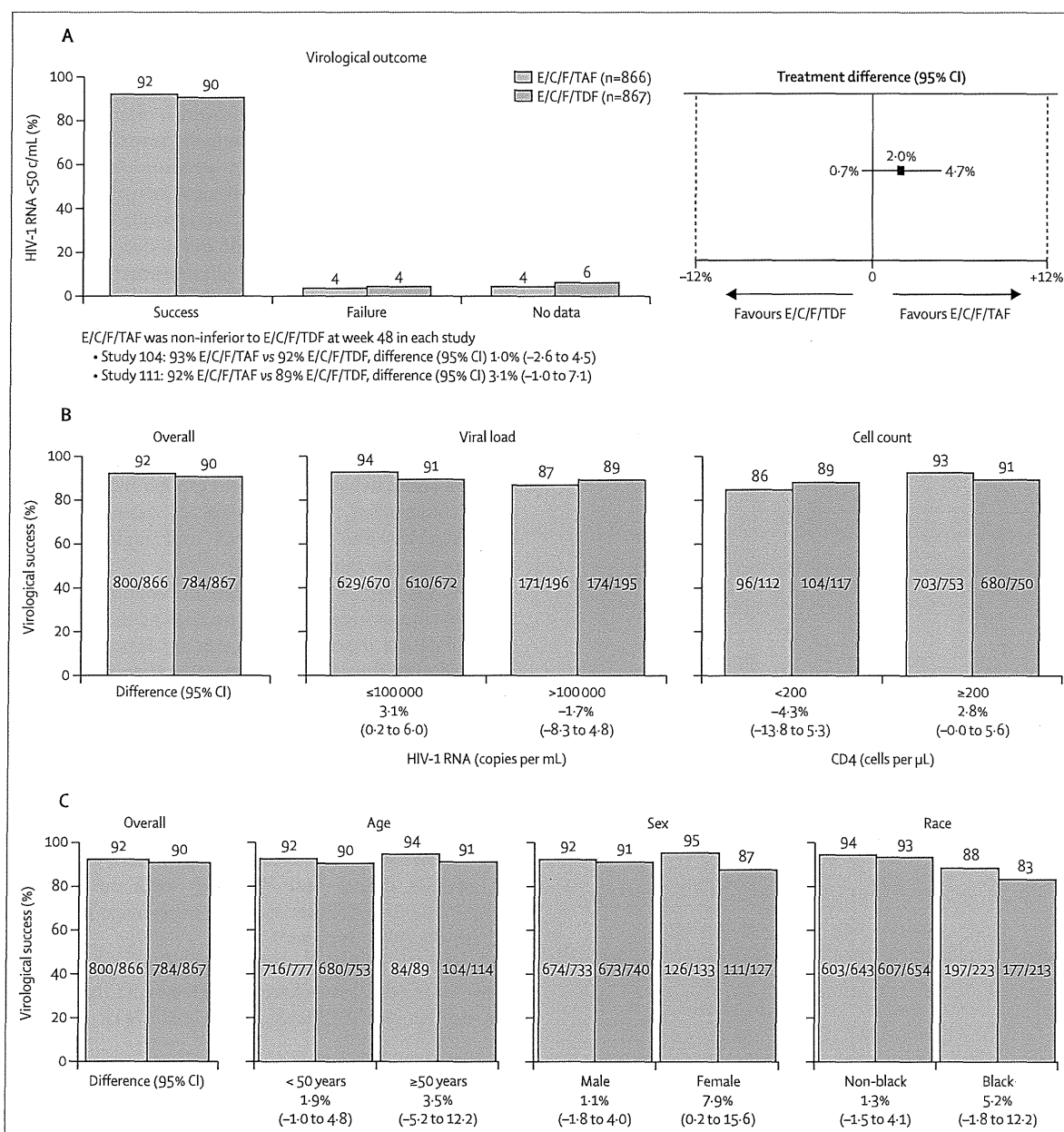

Figure 2: (A) Primary endpoint: HIV-1 RNA <50 copies/mL at week 48, (B) efficacy in baseline HIV-RNA and CD4 subgroups, and (C) efficacy in selected subgroups
E/C/F/TAF=elvitegravir, cobicistat, emtricitabine, tenofovir alafenamide. E/C/F/TDF=elvitegravir, cobicistat, emtricitabine, tenofovir disoproxil fumarate.

concentrations. Bioanalytical analyses of drug concentrations of tenofovir alafenamide and tenofovir in plasma and tenofovir-diphosphate in peripheral blood mononuclear cells were done by QPS (Newark, DE, USA).

Role of the funding source

The funder designed the study, collected and analysed data, interpreted the results, and helped write the report. PES and DW are investigators who had access to the analyzed data, independently interpreted the results, and helped write the report. All authors had access to the

	Elvitegravir, cobicistat, emtricitabine, tenofovir alafenamide (n=866)	Elvitegravir, cobicistat, emtricitabine, tenofovir disoproxil fumarate (n=867)
Diarrhoea	147 (17%)	164 (19%)
Nausea	132 (15%)	151 (17%)
Headache	124 (14%)	108 (13%)
Upper respiratory tract infection	99 (11%)	109 (13%)
Nasopharyngitis	78 (9%)	80 (9%)
Fatigue	71 (8%)	71 (8%)
Cough	67 (8%)	60 (7%)
Vomiting	62 (7%)	54 (6%)
Arthralgia	61 (7%)	39 (5%)
Back pain	60 (7%)	57 (7%)
Insomnia	57 (7%)	48 (6%)
Rash	55 (6%)	46 (5%)
Pyrexia	45 (5%)	41 (5%)
Dizziness	44 (5%)	37 (4%)

Data are n (%).

Table 2: Common adverse events (all grades) in ≥5% of patients

See Online for appendix

analysed data and could assess the results and conclusions. Additional information or analyses were available to any author upon request. PES, DW, SM, MWF, and AKC made the decision to submit the report.

Results

2175 patients were screened for both studies, of whom 1744 were randomly assigned to receive treatment. 1733 received at least one dose of study drug; 866 received E/C/F/tenofovir alafenamide and 867 received E/C/F/ tenofovir disoproxil fumarate (figure 1). Table 1 shows baseline characteristics of participants. E/C/F/tenofovir alafenamide was non-inferior to E/C/F/tenofovir disoproxil fumarate for the combined primary outcome (800 patients [92%] vs 784 patients [90%], adjusted difference 2·0%, 95% CI –0·7% to 4·7%) and for each study (figure 2). With a cutoff of fewer than 20 copies per mL, virological outcome at week 48 by FDA snapshot algorithm was 84·4% for the E/C/F/tenofovir alafenamide group and 84·0% for the E/C/F/tenofovir disoproxil fumarate group (difference in percentages 0·4%, 95% CI –3·0% to 3·8%, p=0·83). Viral suppression was high in both treatment groups for per-protocol analysis (781 [98%] of 801 for E/C/F/ tenofovir alafenamide group and 763 [97%] of 789 patients for E/C/F/tenofovir disoproxil fumarate group, adjusted difference 0·8%, 95% CI –1·0% to 2·5%) and the other the secondary efficacy endpoints (appendix) and for various subgroups (figure 2). We noted significant differences in efficacy for those with fewer than 100 000 copies per mL baseline HIV-1 RNA (94% for E/C/F/tenofovir alafenamide vs 91% for tenofovir disoproxil fumarate, difference in percentage 3·1%, 95% CI 0·2–6·0) and for women (95% for tenofovir alafenamide and 87% for tenofovir disoproxil fumarate, difference in percentage 7·9%, 95% CI 0·2–15·6). The mean increases from baseline in CD4 cell counts were higher for the E/C/F/tenofovir alafenamide group through week 48 (observed data), as follows: E/C/F/tenofovir alafenamide 230 (SD 177·3) cells per mL; E/C/F/tenofovir disoproxil fumarate 211 (170·7) cells per mL; difference in LSM 19 cells per mL, 95% CI: 3 to 36 cells per mL; p=0·024.

We noted virological failure with resistance in seven (0·8%) of 866 patients in the E/C/F/tenofovir alafenamide group versus five (0·6%) of 867 patients in the E/C/F/ tenofovir disoproxil fumarate group (appendix). Resistance mutation development was similar between treatment groups (appendix). All patients with emergent resistance developed the reverse transcriptase mutation, Met184Val/Ile. One patient in the E/C/F/tenofovir alafenamide group and in two patients in E/C/F/tenofovir disoproxil fumarate developed the Lys65Arg reverse transcriptase mutation. Eight of 12 patients (five in the E/C/F/tenofovir alafenamide group and three in the E/C/F/tenofovir disoproxil fumarate group) developed primary INSTI-R, all of which were genotypically
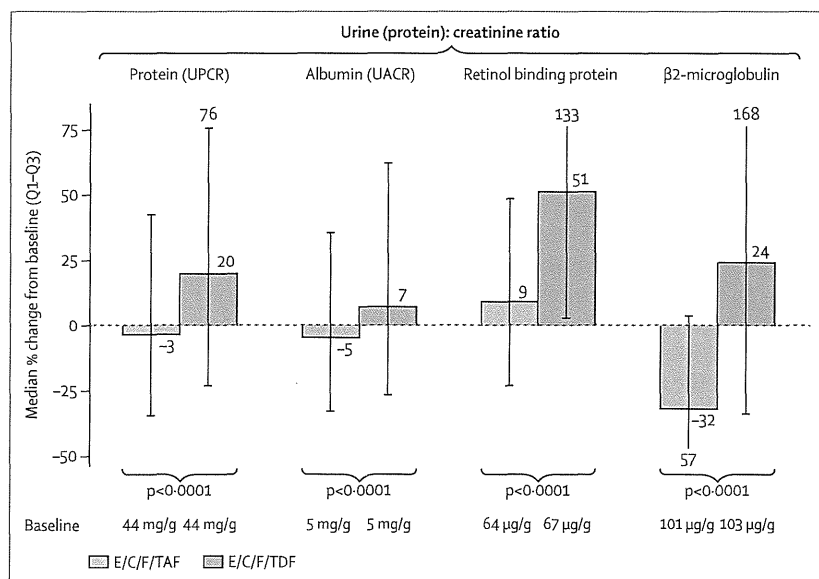

Figure 3: Changes in quantitative proteinuria at week 48
UPCR=urine protein to creatinine ratio. UACR=urine albumin to creatinine ratio. E/C/F/TAF=elvitegravir, cobicistat, emtricitabine, tenofovir alafenamide. E/C/F/TDF=elvitegravir, cobicistat, emtricitabine, tenofovir disoproxil fumarate.
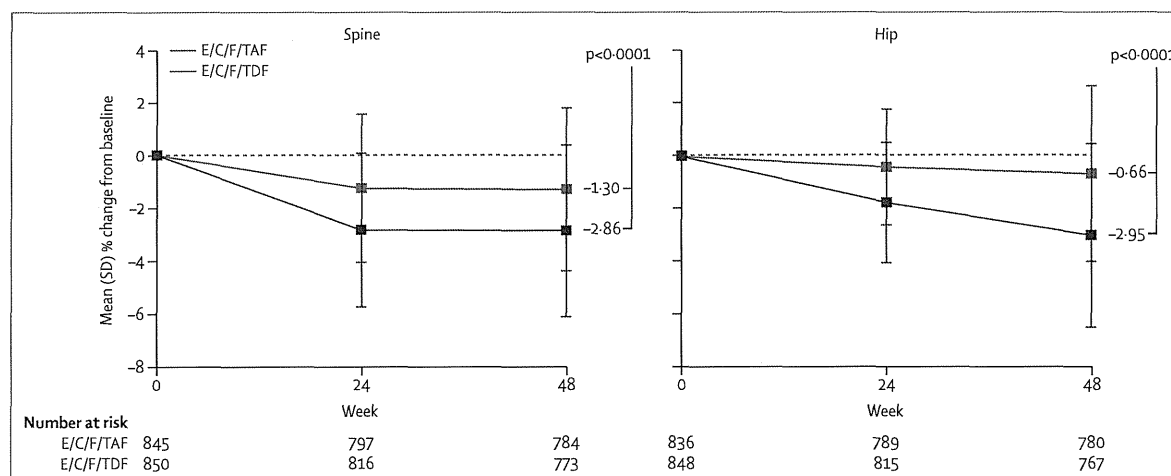
Figure 4: Changes in spine and hip bone mineral density through week 48
E/C/F/TAF=elvitegravir, cobicistat, emtricitabine, tenofovir alafenamide. E/C/F/TDF=elvitegravir, cobicistat, emtricitabine, tenofovir disoproxil fumarate.

susceptible to dolutegravir. We did not record any novel tenofovir resistance mutations in any of the patients given E/C/F/tenofovir alafenamide.

36 participants in the tenofovir alafenamide group and 29 in the E/C/F/tenofovir disoproxil fumarate group participated in the intensive pharmacokinetic substudy; five of those enrolled were women. Of those, 21 patients who received E/C/F/tenofovir alafenamide and 14 who received E/C/F/tenofovir disoproxil fumarate participated in the PBMC substudy. Plasma tenofovir exposure (AUC_{tau}) after administration of E/C/F/tenofovir alafenamide was 91% lower than tenofovir exposure achieved with administration of E/C/F/tenofovir disoproxil fumarate (appendix). The PBMC tenofovir-diphosphate AUC_{tau} was 4·1 times higher in participants receiving E/C/F/tenofovir alafenamide than in those receiving E/C/F/tenofovir disoproxil fumarate.

Both treatments were well tolerated, with most adverse events reported as mild or moderate in severity (appendix). Adverse events leading to study drug discontinuation were uncommon: E/C/F/tenofovir alafenamide 8 (0·9%) and E/C/F/tenofovir disoproxil fumarate 13 (1·5%); adverse events leading to study drug discontinuation deemed related to study drugs were similar: E/C/F/tenofovir alafenamide 7 (0·8%) and E/C/F/tenofovir disoproxil fumarate 11 (1·3%). Table 2 shows adverse events reported by 5% or more of patients in either treatment group. Roughly 20% of patients in either group had a grade 3 or 4 laboratory abnormality (appendix). Five patients died (E/C/F/tenofovir alafenamide two patients, embolic stroke, and alcohol poisoning; E/C/F/tenofovir disoproxil fumarate three patients, cardiac arrest, multiple drug overdose, and myocardial infarction). None of the serious adverse events that resulted in the deaths were deemed related to study drugs by the investigator.

There were no discontinuations due to renal adverse events in the E/C/F/tenofovir alafenamide group.

Four patients in the E/C/F/tenofovir disoproxil fumarate group discontinued study drug because of renal adverse events. Three patients had decreased glomerular filtration rate and another patient developed nephropathy, all believed to be related to study drug. We noted no cases of proximal renal tubulopathy (including Fanconi syndrome) in either treatment group. We recorded decreases from baseline in mean estimated glomerular filtration rate by week 2 with no further change thereafter. We noted significantly smaller decreases in estimated glomerular filtration rate in the E/C/F/tenofovir alafenamide group than in the E/C/F/tenofovir disoproxil fumarate group (appendix). At 48 weeks, quantitative proteinuria (total urinary protein, albumin, retinol binding protein and β2-microglobulin to urine creatinine ratios) increased from baseline in the E/C/F/tenofovir disoproxil fumarate group; reductions or significantly smaller increases in these urinary proteins were noted in the E/C/F/tenofovir alafenamide group (figure 3). Other measures of proximal renal tubular function (fractional excretion of phosphate and uric acid) showed significantly less change in patients receiving E/C/F/ tenofovir alafenamide compared with the E/C/F/ tenofovir disoproxil fumarate group (data not shown).

Fractures were uncommon in both treatment groups (one in the E/C/F/tenofovir alafenamide group and seven in the E/C/F/tenofovir disoproxil fumarate group), and deemed by the investigator to be the result of trauma and unrelated to the study drugs; none resulted in permanent discontinuation of study drugs. Patients in the E/C/F/ tenofovir alafenamide group had significantly less reduction in bone mineral density than those in the E/C/F/tenofovir disoproxil fumarate group through 48 weeks (figure 4). Decrease in bone mineral density was significantly lower in the E/C/F/tenofovir alafenamide group for both lumbar spine (mean –1·30% [SD 3·08] vs –2·86 [3·25]; p<0·0001) and total hip (–0·66 [3·26] vs

−2·95 [3·41], p<0·0001; figure 3). Roughly one-third as many patients in the E/C/F/tenofovir alafenamide had more than 3% bone loss at the hip (E/C/F/tenofovir alafenamide 131/780 [16·8%]; E/C/F/tenofovir disoproxil fumarate 384/767 [50·1%]), and about half as many patients in the E/C/F/tenofovir alafenamide group had more than 3% bone loss at the spine (E/C/F/tenofovir alafenamide 208/784 [26·5%]; E/C/F/tenofovir disoproxil fumarate 354/773 [45·8%]; appendix).

We recorded greater increases in the fasting lipid parameters total cholesterol, direct low-density lipoprotein, high-density lipoprotein, and triglycerides, but identical changes in total cholesterol to high-density lipoprotein ratio, in patients given E/C/F/tenofovir alafenamide compared with those given E/C/F/tenofovir disoproxil fumarate at week 48 (appendix). 31 (3·6%) of 866 of patients given E/C/F/tenofovir alafenamide and 25 (2·9%) of 867 of participants given E/C/F/tenofovir disoproxil fumarate started lipid-lowering drugs (p=0·42).

Discussion

In these two randomised phase 3 clinical trials, we show that the novel tenofovir prodrug, tenofovir alafenamide achieved a high rate of virological suppression when given as part of a coformulated tablet that included emtricitabine, elvitegravir, and cobicistat. The response was non-inferior to the control group, which consisted of the approved single tablet regimen of elvitegravir, cobicistat, emtricitabine, and tenofovir disoproxil fumarate. The results were mostly non-inferior between the two groups irrespective of baseline demographic or clinical characteristics, although outcome was significantly better for tenofovir alafenamide in women and in those who had baseline viral loads lower than 100000 copies per mL. CD4 cell count increases at week 48 were significantly greater in the tenofovir alafenamide group than in the tenofovir disoproxil fumarate group. Both coformulations were well tolerated and discontinuations for drug-related adverse events were rare in both study groups.

The high rates of successful treatment (92% in the E/C/F/tenofovir alafenamide group and and 90% in the E/C/F/tenofovir disoproxil fumarate group) marks the first time that both treatment groups in a fully powered comparative clinical trial exceeded the 90% threshold for virological suppression (plasma HIV-1 RNA <50 copies per mL) using the snapshot analysis at 48 weeks. Virological failure was infrequent in both groups, arising in 3·6% of paitents given E/C/F/tenofovir alafenamide and 4·0% of patients given E/C/F/tenofovir disoproxil fumarate. Although resistance to study treatment was not recorded in the E/C/F/tenofovir alafenamide group of the phase 2 trial, in these two larger studies a small percentage of patients (<1% in both groups) did develop drug resistance to some of the treatments, most commonly the nucleoside reverse transcriptase inhibitor mutation Met184Val selected by emtricitabine.

The high virological suppression recorded in these studies reinforces the extraordinary effectiveness of contemporary HIV treatment. With prolonged virological suppression, improved clinical outcomes, and longer survival,[16] patients will potentially be exposed to antiretroviral agents for decades. As a result, maximising the safety of drugs used for HIV remains a high priority, and long-term renal and bone safety are important considerations. Although generally well tolerated as initial treatment, findings of several studies have shown an association between tenofovir disoproxil fumarate and kidney disease. A meta-analysis[17] of prospective studies of HIV treatments showed a significantly greater loss of kidney function in patients receiving tenofovir disoproxil fumarate-based treatments versus non-tenofovir disoproxil fumarate regimens; a higher risk of acute renal failure was also noted. In a large cohort analysis from the Veterans Health Administration, tenofovir exposure was independently associated with proteinuria, rapid estimated glomerular filtration rate decrease, and the development estimated glomerular filtration rate less than 60 mL per min.[18] Commonly cited risk factors for tenofovir disoproxil fumarate-related nephrotoxicity include older age, co-administration with ritonavir-boosted protease inhibitors (which further increase tenofovir plasma levels), and other comorbidities associated with renal disease.[4]

There is an increased prevalence of osteopenia and osteoporosis in patients with HIV infection.[19] The cause is multifactorial, with both HIV disease-specific and treatment-specific effects observed. Generally, initiation of antiretroviral therapy leads to a reduction in bone mineral density,[20] possibly related to immune reconstitution.[21] This effect is larger in patients receiving tenofovir disoproxil fumarate and certain protease-inhibitor based regimens.[5,22] The mechanism of tenofovir disoproxil fumarate-related reductions in bone mineral density is poorly understood but might include osteomalacia as a result of increased urinary phosphate loss.[23]

In these two clinical trials, protocol-specified renal and bone endpoints confirmed the favourable safety and tolerability profile of tenofovir alafenamide reported in earlier studies. Although no particpants had overt renal failure or clinically significant tubulopathy, patients given tenofovir alafenamide had smaller reductions in estimated glomerular filtration rate and more favourable changes in urine protein to creatinine and urine albumin to creatinine ratios. Specific markers of proximal renal tubular dysfunction, including urinary retinol binding protein, urinary β2-microglobulin, fractional excretion of uric acid, and fractional excretion of phosphate all significantly favoured the tenofovir alafenamide over the tenofovir disoproxil fumarate group, suggesting a lower potential for nephrotoxicity with tenofovir alafenamide than with tenofovir disoproxil fumarate.

The present studies represent the largest bone mineral density dataset in patients with HIV up to now. Treatment

with E/C/F/tenofovir alafenamide resulted in significantly smaller reductions in bone mineral density at both the hip and the lumbar spine at week 48. The magnitude of bone mineral density decline recorded in the tenofovir alafenamide group at the hip (0·7%) similar to that seen in randomised studies of treatment-naive patients on nucleoside or nucleotide-sparing regimens.[24,25] Furthermore, with a 3% threshold for the least significant change to account for the imprecision of repeat dual energy x-ray absorptiometry measures,[26] 27% of patients in the tenofovir alafenamide group versus 46% in the tenofovir disoproxil fumarate group exceeded this threshold at the spine, and 17% versus 50% at the hip.

Treatment with tenofovir disoproxil fumarate has consistently been associated with less increase in lipids compared with other regimens in treatment-naive patients. The independent effect of tenofovir on lipids was most clearly shown in a study that added tenofovir disoproxil fumarate to stable background treatment in virologically suppressed patients;[27] findings showed a significant reduction in total, LDL, and non-HDL cholesterol levels. In both the phase 2 comparative study of tenofovir alafenamide vs tenofovir disoproxil fumarate and the larger phase 3 studies presented here, increases in total, LDL, and HDL cholesterol, and triglycerides, were greater in the tenofovir alafenamide than the tenofovir disoproxil fumarate group. However, the difference in total cholesterol to HDL ratio at week 48 was not significantly different between treatment groups, and a small and similar proportion of participants (<4%) initiating lipid-modifying agents.

The net favourable effects on renal and bone parameters for tenofovir alafenamide almost certainly relates to the lower plasma levels of tenofovir recorded in those receiving tenofovir alafenamide instead of tenofovir disoproxil fumarate. In a pharmacokinetic substudy, plasma tenofovir exposure was 90% lower in the tenofovir alafenamide than in the tenofovir disoproxil fumarate group. Conversely, the intracellular concentration of the active metabolite, tenofovir diphosphate, was four times higher. The ability to achieve higher intracellular concentrations enables a markedly lower daily dose of tenofovir alafenamide (10 mg with ritonavir or cobicistat) versus tenofovir disoproxil fumarate (300 mg) while achieving a similar or greater antiviral effect.[11] This lower dose of tenofovir alafenamide will help with both a broader range of coformulations and reduce the cost of manufacturing of the compound, the latter an important consideration in resource-limited settings. In addition to the coformulation E/C/F/tenofovir alafenamide, tenofovir alafenamide is being studied in various fixed dose combinations for HIV (with emtricitabine, with rilpivirine and emtricitabine, and with darunavir, cobicistat, and emtricitabine), and as a single agent for hepatitis B virus.

Strengths of these two studies include the large overall sample size, the randomised blinded study design with one variable of tenofovir alafenamide verus tenofovir disoproxil fumarate, and protocol-specified renal and bone endpoints. Additionally, study sites were geographically diverse, as was the ethnic origin of the participants enrolled. Limitations include a low power to assess rare clinical safety events such as renal adverse events and fractures in patients with limited baseline risk factors for kidney and bone disease, a small proportion of study participants with advanced HIV disease, a small proportion of women participants, and the exclusion of patients with chronic hepatitis B virus infection. The efficacy of tenofovir alafenamide in the treatment of chronic hepatitis B monoinfection, as well as HIV and hepatitis B virus co-infection, is currently being studied. Additionally, a clinical trial of women (NCT01705574) will give substantially more information about the efficacy, tolerability, and pharmacokinetic parameters of tenofovir alafenamide in women with HIV. Importantly, the efficacy of tenofovir alafenamide alone, or in combination with emtricitabine, for prevention, such as pre-exposure prophylaxis, is unknown and currently being explored.

In summary, in these two randomised clinical trials, treatment with a coformulated tablet of E/C/F/tenofovir alafenamide provided non-inferior virological suppression to an already approved and guidelines-recommended tablet of E/C/F/tenofovir disoproxil fumarate. Compared with tenofovir disoproxil fumarate, the nucleotide reverse transcriptase inhibitor tenofovir alafenamide showed significantly more favourable effects on renal and bone parameters. All these effects were probably related to the markedly lower plasma concentrations of tenofovir reported with tenofovir alafenamide compared with tenofovir disoproxil fumarate. Although the long-term clinical significance of these findings is unknown, it is reasonable to expect that these results will translate into improved safety of tenofovir alafenamide-based antiretroviral therapy over years of treatment while maintaining a similarly high efficacy rate.